

CLOSURE RELATIONS FOR E^\pm PAIR-SIGNATURES IN GAMMA-RAY BURSTSKOHTA MURASE¹ AND KUNIHITO IOKA^{2,3}

ABSTRACT

We present recipes to diagnose the fireball of gamma-ray bursts (GRBs) by combining observations of e^\pm pair-signatures (the pair-annihilation line and the cutoff energy due to the pair-creation process). Our recipes are largely model-independent and extract information even from the non-detection of either pair-signature. We evaluate physical quantities such as the Lorentz factor, optical depth and pair-to-baryon ratio, only from the observable quantities. In particular, we can test whether the prompt emission of GRBs comes from the pair/baryonic photosphere or not. The future-coming Gamma-Ray Large Area Space Telescope (GLAST) satellite will provide us with good chances to use our recipes by detecting or non-detecting pair-signatures.

Subject headings: gamma rays: bursts — gamma rays: theory — plasmas

1. INTRODUCTION

Gamma-ray burst (GRB) is one of the most mysterious objects in the universe. Various models are suggested, but no conclusive picture has been obtained (see reviews, e.g., Mészáros 2006; Zhang 2007). One of the leading models is the optically thin internal shock model, where the prompt emission is explained by electromagnetic radiation from relativistic electrons accelerated in the internal shocks (see, e.g., Rees & Mészáros 1994). One of the other leading models is the photospheric emission model, where the prompt emission comes from the photospheric radius r_{ph} at which the Thomson optical depth is unity, i.e., $\tau = 1$ (see, e.g., Rees & Mészáros 2005). The possibility that a fireball contains copious e^\pm pairs (a pair-dominated fireball) is also discussed by many authors. In particular, we recently proposed that the pair photosphere is unstable and capable of making the observed non-thermal spectrum with high radiative efficiency (Ioka et al. 2007). The existence of copious pairs can extend the photosphere compared to baryonic photosphere which is determined by baryon-related electrons. Such pairs could be produced via dissipation processes such as internal shocks and magnetic reconnection.

Prompt gamma-rays are typically radiated at ~ 100 keV. Observationally, even more high-energy photons were detected by the EGRET detector. Such high-energy emissions are theoretically expected due to radiation processes such as the synchrotron and/or inverse Compton emission. Sufficiently high-energy photons cannot avoid the pair-production process, which leads to the existence of the cutoff energy due to pair-creation. On the other hand, there may be a lot of pairs that can be seen as pair-annihilation lines via the pair-annihilation process (Ioka et al. 2007; Pe’er & Waxman 2004; Pe’er et al. 2006). Future-coming GLAST satellite is the suitable detector to observe such pair-signatures, a pair-annihilation line and/or cutoff energy.

Obviously, such pair-signatures (the pair-annihilation line and the cutoff energy due to the pair-creation process) have important information on the fireball of GRBs. For example, the cutoff energy due to pair-creation has information on the bulk Lorentz factor of a fireball. This possibility has already

been investigated by several authors (Baring & Harding 1997; Lithwick & Sari 2001; Razzaque et al. 2004). However, there are few studies focusing on both of the pair-annihilation line and the cutoff energy due to pair-creation.

In this paper, we clarify that, combining both of pair-signatures, we can get much information about the GRB fireball (§ 2). Even if we can not detect either of pair-signatures, the non-detection itself gives information (§ 3). We show that observations of pair-signatures allow us to evaluate the Lorentz factor, optical depth of a fireball and pair-to-baryon ratio and so on. In particular, we derive these relations only from the observable quantities and make discussions as model-independently as possible. Our recipes are especially profitable to test the pair photospheric emission model (§ 4).

Throughout the paper, we shall assume that we know the gamma-ray spectrum in the wide energy range (e.g., the high-energy spectral index β and so on), source redshift z from other observations, and hence the luminosity $\varepsilon L_\varepsilon$ at given observed energy ε from the observed flux (see Fig. 1).

2. DIAGNOSING THE FIREBALL BY E^\pm PAIR-SIGNATURES

Let us assume that we can find a pair-annihilation line in the spectrum of the prompt emission (Fig. 1), which typically peaks at

$$\varepsilon_{\text{ann}} \simeq \frac{\Gamma}{1+z} m_e c^2. \quad (1)$$

The above expression is valid as long as pairs forming a pair-annihilation line are non-relativistic. This is a reasonable assumption because the cooling time of sufficiently relativistic pairs t_{cool} due to the magnetic and/or photon fields is usually much shorter than the pair-annihilation time t_{ann} . However, we have to note that the line would be broadened by dispersion of the Doppler factor. Therefore, gamma-rays due to pair-annihilation will be observed as a “bump” rather than a “line”. There are several possible reasons that make line-broadening. First, the order-of-unity distribution of the Lorentz factor in the emission region can make the line broadened by order-of-unity even when pairs are non-relativistic in the comoving frame. Second, the order-of-unity line-broadening is also caused by the fact that we observe a section of the emission region with the opening angle $\sim 1/\Gamma$ rather than a small spot. The Doppler factor towards the observer is different by order-of-unity between the center and the edge of the observed emission region. Third, the order-of-unity variation of the Lorentz factor may

¹ YITP, Kyoto University, Kyoto, 606-8502, Japan

² Department of Physics, Kyoto University, Kyoto 606-8502, Japan

³ Theory Division, KEK (High Energy Accelerator Research Organization), 1-1 Oho, Tsukuba 305-0801, Japan

also occur within the dynamical time. The recent observations may suggest the emission is radiatively very efficient (Ioka et al. 2006; Zhang et al. 2007). The efficient internal dissipation may make the fireball radiation-dominated. If so, the Lorentz factor increases as $\Gamma \propto r$, and the Lorentz factor varies by order-of-unity within the dynamical time. Therefore, we can expect that all the three effects broaden the line by order-of-unity.

The total luminosity of the pair-annihilation line L_{ann} (Coppi & Blandford 1990; Svensson 1982), the kinetic luminosity of pairs L_{\pm} and the kinetic luminosity of baryons L_p are given by

$$L_{\text{ann}} \simeq \frac{3}{8} n_+ n_- \sigma_T c (2m_e c^2) (4\pi r^2 \Delta') \Gamma^2, \quad (2)$$

$$L_{\pm} = n_{\pm} c (2m_e c^2) (4\pi r^2) \Gamma^2, \quad (3)$$

$$L_p = n_p c (m_p c^2) (4\pi r^2) \Gamma^2, \quad (4)$$

respectively. Here r is the emission radius, Δ' is the comoving width of the emission region, and $n_+ = n_{\pm}$, $n_- = n_{\pm} + n_p$, n_{\pm} and n_p are the comoving density of positrons, electrons, e^{\pm} pairs and baryon-related electrons, respectively. We have assumed that most of the sufficiently relativistic pairs cool down in the dynamical time. Combining expressions of L_{ann} and L_{\pm} leads to

$$L_{\text{ann}} \simeq \frac{3}{16} L_{\pm} \tau_{\pm} \left(1 + \frac{n_p}{n_{\pm}} \right), \quad (5)$$

where $\tau_{\pm} \simeq 2n_{\pm} \sigma_T \Delta'$ denotes the optical depth against pairs.

Pair-creation processes such as $\gamma\gamma \rightarrow e^+e^-$ and $e\gamma \rightarrow ee^+e^-$ prevent sufficiently high-energy photons from escaping the source. Usually, the most important pair-creation process is $\gamma\gamma \rightarrow e^+e^-$ (Razzaque et al. 2004). The optical depth for this process $\tau_{\gamma\gamma}$ at some energy ε can be evaluated for a given photon spectrum. The elaborate evaluation of $\tau_{\gamma\gamma}$ is possible if we know the spectrum in detail (see, e.g., Coppi & Blandford 1990; Baring 2006; Baring & Harding 1997; Gupta & Zhang 2007). Here, we shall assume a power-law photon spectrum for simplicity, i.e., with the luminosity $\varepsilon L_{\varepsilon}(\varepsilon) = L_0 (\varepsilon/\varepsilon_0)^{2-\beta}$ for $\beta > 2$. Then, we have (Gould & Schröder 1967; Lightman & Zdziarski 1987; Svensson 1987; Lithwick & Sari 2001; Baring 2006)

$$\tau_{\gamma\gamma}(\varepsilon) \simeq \xi(\beta) n_{\gamma}(\varepsilon_{\gamma} > \tilde{\varepsilon}) \sigma_T \Delta', \quad \left[\tilde{\varepsilon} = \frac{(\Gamma m_e c^2)^2}{(1+z)^2 \varepsilon} \right], \quad (6)$$

where the comoving density of photons whose energies are larger than $\tilde{\varepsilon}$ is given by

$$n_{\gamma}(\varepsilon_{\gamma} > \tilde{\varepsilon}) = \frac{L_0}{4\pi r^2 \Gamma c \varepsilon_0 (1+z)} \int_{\tilde{\varepsilon}} \frac{d\varepsilon_{\gamma}}{\varepsilon_0} \left(\frac{\varepsilon_{\gamma}}{\varepsilon_0} \right)^{-\beta}, \quad (7)$$

and $\tilde{\varepsilon}$ is the energy of a photon which interacts with the photon of energy ε at the pair-creation threshold. $\xi(\beta)$ is the numerical factor which depends on the photon index (Gould & Schröder 1967; Lightman & Zdziarski 1987; Svensson 1987; Coppi & Blandford 1990; Lithwick & Sari 2001; Baring 2006; Gupta & Zhang 2007). $\xi(\beta)/(\beta-1)$ decreases with β , and its values are $\xi(\beta) = 11/90 \simeq 0.12$ and $\xi(\beta) = 7/75 \simeq 0.093$ for $\beta = 2$ and 3, respectively⁴. For the isotropic photon distribution with an

infinite power-law, we can use $\xi(\beta) \simeq 7(\beta-1)/(6\beta^{5/3}(\beta+1))$ for $1 < \beta < 7$ (Svensson 1987; Baring 2006). Note that L_0 is related to the observed (time-resolved) flux $\varepsilon F_{\varepsilon}(\varepsilon)$ by

$$\varepsilon F_{\varepsilon}(\varepsilon = \varepsilon_0) = \frac{L_0}{4\pi d_L^2}, \quad (8)$$

where d_L is the luminosity distance to the source. Unless a fireball is completely thin, where all the photons can escape without attenuation, the cutoff energy ε_{cut} exists due to the pair-creation process $\gamma\gamma \rightarrow e^+e^-$, where $\tau_{\gamma\gamma}(\varepsilon_{\text{cut}}) = 1$ (Fig. 1). With Eq. (3), $\tau_{\gamma\gamma}(\varepsilon_{\text{cut}}) = 1$ is rewritten as

$$1 = \tau_{\gamma\gamma}(\varepsilon_{\text{cut}}) \simeq \frac{L_0}{L_{\pm}} \tau_{\pm} f(\varepsilon_{\text{cut}}, \Gamma), \quad (9)$$

where

$$f(\varepsilon_{\text{cut}}, \Gamma) \simeq \xi(\beta) \frac{\Gamma m_e c^2}{(1+z)\varepsilon_0} \int_{\tilde{\varepsilon}_{\text{cut}}} \frac{d\varepsilon_{\gamma}}{\varepsilon_0} \left(\frac{\varepsilon_{\gamma}}{\varepsilon_0} \right)^{-\beta}. \quad (10)$$

Note that we may arbitrarily take ε_0 by adjusting L_0 . We also note that ε_{cut} is larger than ε_{ann} , as long as ε_{cut} is determined by the pair-creation process $\gamma\gamma \rightarrow e^+e^-$ (and we have also assumed that electrons and positrons are accelerated enough to emit high-energy photons with $\varepsilon > \varepsilon_{\text{cut}}$ via e.g., synchrotron or inverse Compton radiation processes). This is because an assumed photon spectrum has $\beta > 1$ (which is typically expected for prompt emissions), hence the photon number density decreases with photon energies. Therefore, photons with $\varepsilon \lesssim \varepsilon_{\text{ann}}$ do not have enough target photons with $\tilde{\varepsilon} \gtrsim \varepsilon_{\text{ann}}$ in order to be attenuated at $\varepsilon_{\text{cut}} \lesssim \varepsilon_{\text{ann}}$. Otherwise, the created pairs would make the optical depth τ larger than unity. In this case, the cutoff energy is determined by the Compton down-scattering process rather than the pair-creation process for the assumed spectrum (see, e.g., Lithwick & Sari 2001). Although we will hereafter focus on cases where ε_{cut} is determined by the pair-creation cutoff, there are possibilities of $\varepsilon_{\text{cut}} \lesssim \varepsilon_{\text{ann}}$ for $\tau \gtrsim 1$. We may be able to check $\varepsilon_{\text{cut}} \lesssim \varepsilon_{\text{ann}}$ and $\tau \gtrsim 1$, if we can observe the Lorentz factor Γ by other means as well as the cutoff energy ε_{cut} . We would expect that high-energy gamma rays come from the region where $\tau \sim 1$, as long as the dissipation continues until $r \sim r_{\text{ph}}$ and the emission from $r \sim r_{\text{ph}}$ is not negligible. This is because high-energy gamma rays from the region where $\tau \gg 1$ are significantly down-scattered. We would also expect that the GRB radiative efficiency is small (contrary to the observations) if the prompt emission comes only from $\tau \gg 1$ since almost all energy goes into the afterglow. We also note that in some models like the slow dissipation scenario (Ghisellini & Celotti 1996) high-energy photons with $\varepsilon > \varepsilon_{\text{cut}}$ may not be produced because electrons and positrons are not accelerated enough (Pe'er et al. 2006).

2.1. Closure Relations for the Pair-Dominated Fireball

Now, let us assume the pair-dominated fireball, $n_p < 2n_{\pm}$, in this subsection. Then we can solve Eqs. (5) and (9) for the

⁴ When we assume the isotropic photon spectrum with an infinite power-law, we have $\xi(\beta = 2) = 11/90 \simeq 0.12$. This value is obtained by various

authors, e.g., Gould & Schröder (1967), Svensson (1987), Baring (2006) and Gupta & Zhang (2007). Lithwick & Sari (2001) adopt a factor two smaller value as is pointed in Zhang & Mészáros (2001).

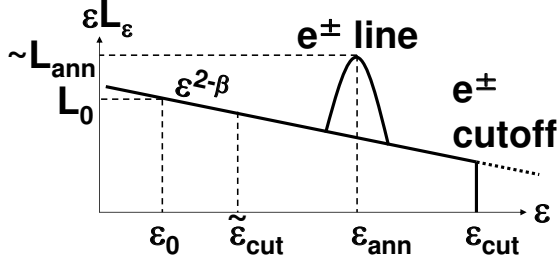


FIG. 1.— The schematic picture of the GRB spectrum showing the observable quantities of pair-signatures [L_{ann} , L_0 , ϵ_0 , ϵ_{cut} , $\epsilon_{\text{ann}} \simeq \Gamma m_e c^2 / (1+z)$ and β]. The recipes to constrain physical quantities of the GRB fireball only with the observable quantities are the followings. (I) The case where we can observe both of the pair-annihilation line and the cutoff energy due to pair-creation, i.e., ϵ_{ann} , L_{ann} and ϵ_{cut} ; If we also obtain the kinetic luminosity of baryons L_p , we can measure τ , τ_\pm and n_\pm/n_p from Eqs. (14), (16) and (17). Without L_p , we obtain the inequalities (18) from $L_p > 0$, while we have an upper limit on τ as well as lower limits on τ_\pm and n_\pm/n_p from the assumption $L_p \lesssim L_\gamma$ by replacing L_p with L_γ in Eqs. (14), (16) and (17). If the inequality (13) is satisfied, the fireball is pair-dominated, $\tau \approx \tau_\pm$, and we can use Eqs. (11) and (12) instead of Eqs. (14) and (15). (II) The case where we only observe ϵ_{cut} , not L_{ann} and ϵ_{ann} ; With L_p , we can give upper limits on τ , n_\pm/n_p and τ_\pm by replacing L_{ann} with $L_0(\Gamma m_e c^2 / (1+z)\epsilon_0)^{2-\beta}$ in Eqs. (14), (16) and (17). Without L_p , we obtain the inequality (20) from $L_p > 0$, while we have an upper limit on τ from $L_p \lesssim L_\gamma$ by replacing L_p and L_{ann} with L_γ and $L_0(\Gamma m_e c^2 / (1+z)\epsilon_0)^{2-\beta}$, respectively, in Eq. (14). $\Gamma (< (1+z)\epsilon_{\text{cut}}/m_e c^2)$ should be acquired by other means. (III) The case where we only observe L_{ann} and ϵ_{ann} , not ϵ_{cut} ; We regard the observed maximum energy ϵ_{max} as the lower limit on the true cutoff energy ϵ_{cut} . With L_p , we can give upper limits on τ and τ_\pm as well as a lower limit on n_\pm/n_p by replacing f_{cut} with $f_{\text{max}} \equiv f(\epsilon_{\text{max}}, \Gamma)$ in Eqs. (14), (16) and (17). Without L_p , we obtain the inequality (22) from $L_p > 0$, while we obtain an upper limit on τ as well as a lower limit on n_\pm/n_p from $L_p \lesssim L_\gamma$ by replacing L_p and f_{cut} with L_γ and f_{max} , respectively, in Eqs. (14) and (16). Such arguments can be also applied to the completely thin fireballs. (IV) The recipes (I)-(III) are especially valuable to test the pair photospheric emission model. The inequalities (18), (20) and (22) are useful to constrain τ_\pm . This model gives $\tau_\pm \sim 1$ in the case (I), and Eq. (24) if L_{ann} is comparable to the underlying continuum emission. The photospheric radius can be also estimated.

two unknown quantities τ_\pm and L_\pm as

$$\tau \approx \tau_\pm \simeq \left(\frac{16}{3} \frac{L_{\text{ann}}}{L_0 f(\epsilon_{\text{cut}}, \Gamma)} \right)^{1/2} \quad (11)$$

$$L_\pm \simeq \left(\frac{16}{3} L_0 L_{\text{ann}} f(\epsilon_{\text{cut}}, \Gamma) \right)^{1/2}. \quad (12)$$

Remarkably, the above two quantities are expressed only by the observable quantities [L_{ann} , L_0 , ϵ_0 , ϵ_{cut} , $\epsilon_{\text{ann}} \simeq \Gamma m_e c^2 / (1+z)$ and β], so that we can evaluate $\tau_\pm \approx \tau$ and L_\pm . Note that we have not assumed the frequently used relation $r \simeq 2\Gamma\Delta'$, which is expected in the internal shock model. Because we have not specified the model, our recipes are largely model-independent in that sense. The absence of σ_T in Eqs. (11) and (12) just comes from the fact that the pair-annihilation, pair-creation and Compton scattering are all basic two-body interaction processes with cross section $\sim \sigma_T$. Ambiguities arising from the transformation between the comoving frame and observer frame are canceled, because the transformation between the two frames is the same for L_0 , L_\pm and L_{ann} .

Eqs. (11) and (12) are useful because they enable us to estimate $\tau \approx \tau_\pm$ and L_\pm from observational quantities only, although there will be possible uncertainties due to, e.g., observational difficulties in evaluation of ϵ_{cut} , ϵ_{cut} and L_{ann} . In Figs. 2 and 3, we demonstrate that we can obtain information on τ for a given burst (especially a given pulse). Observations of pair-signatures will enable us to plot the point in such a figure and to compare it with lines expressing optical depths. Of

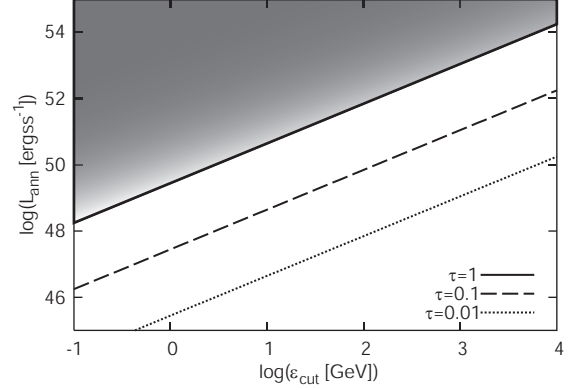


FIG. 2.— The relation between the cutoff energy ϵ_{cut} and total luminosity of a pair annihilation line L_{ann} for given optical depths τ . Lines are calculated by exploiting Eqs. (10) and (14). Used parameters are $L_p = 10^{50}$ ergs s^{-1} , $L_0 = 10^{51}$ ergs s^{-1} , $\epsilon_0 = 10^{2.5}$ keV, $\Gamma = 10^{2.5}$, $\beta = 2.2$ and $z = 0.1$. In this case, the fireball is pair-dominated on this figure, and we can use Eq. (11) instead of Eq. (14). The shaded region expresses $\tau \gtrsim 1$, where photons suffer from Compton scatterings. If we can obtain necessary quantities such as L_{ann} in Fig. 1, we can estimate τ by plotting observational quantities in this figure. Note that ϵ_{cut} should be larger than $\epsilon_{\text{ann}} \simeq \Gamma m_e c^2 / (1+z)$ for typical photon spectra as long as ϵ_{cut} is determined by the pair-creation process.

course, a line for a given τ is different among bursts with different parameter sets. However, we could see the tendency of the distribution of the optical depth for some bursts (or pulses) with a similar parameter set. In this case, lines for a given optical depth can be expressed as "a band" with a finite width. We think that the plot without lines for optical depths may be also useful. More and more observations of pair-signatures will allow us to plot points with optical depths in the $\epsilon_{\text{cut}} - L_{\text{ann}}$ plane.

The assumption $n_p < 2n_\pm$ can be checked posteriorly by the observations. From Eqs. (3) and (4), we have the condition for the fireball to be pair-dominated,

$$\frac{m_p L_\pm}{m_e L_p} \simeq \frac{2n_\pm}{n_p} > 1, \quad (13)$$

which may be checked if we can measure L_p from other observations. For example, we could obtain $L_p \sim L_p^{\text{AG}}$, where L_p^{AG} is the kinetic luminosity of baryons estimated from the afterglow observations. Note that the inequality (13) just means that the pair photospheric radius should be larger than the baryonic photospheric radius, i.e., $r_{\text{ph},\pm} > r_{\text{ph},p}$. Especially, we have a closure relation $\tau_\pm \simeq 1$ for prompt emissions coming from a pair photosphere.

The kinetic luminosity of baryons may be usually less than the observed gamma-ray luminosity, $L_p \lesssim L_\gamma$, as inferred by recent observations that the prompt emission is radiatively very efficient (Ioka et al. 2006; Zhang et al. 2007). It is not very convincing yet since we cannot measure the precise GRB energy at present. But once it is observationally established, we obtain the useful sufficient condition. If the sufficient condition, $m_p L_\pm / m_e L_\gamma > 1$, is satisfied, we can justify the pair-dominance in the inequality (13) by observations. This sufficient condition will be useful as we do not need to evaluate L_p .

2.2. More General Relations

As shown in previous subsections, signatures of pair-annihilation and -creation are useful as a diagnostic tool of the pair-dominated fireball in GRBs. However, the fireball could not be pair-dominated, where the inequality (13) is not satis-

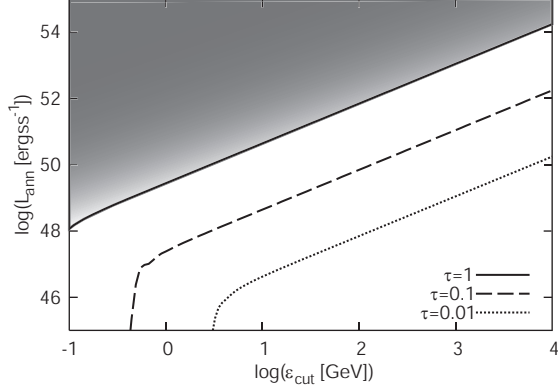


FIG. 3.— The same as Fig. 2, but for $L_p = 10^{52}$ ergs s^{-1} . In this case, the fireball is not pair-dominated for sufficiently small ϵ_{cut} , given fixed τ . When the fireball is baryon-dominated, we cannot expect a pair-annihilation line. As pairs become dominant, L_{ann} increases sharply.

fied. Taking into account of the term $n_p/n_{\pm} \simeq 2m_e L_p/m_p L_{\pm}$ in Eq. (5), we can derive the quadratic equation for L_{\pm} from Eqs. (5) and (9), and generalize Eqs. (11) and (12) as

$$\tau \simeq \left(\frac{16}{3} \frac{L_{\text{ann}}}{L_0 f_{\text{cut}}} + \frac{m_e^2 L_p^2}{m_p^2 L_0^2 f_{\text{cut}}^2} \right)^{1/2}, \quad (14)$$

$$L_{\pm} \simeq \left(\frac{16}{3} L_0 L_{\text{ann}} f_{\text{cut}} + \frac{m_e^2}{m_p^2} L_p^2 \right)^{1/2} - \frac{m_e}{m_p} L_p, \quad (15)$$

where we have defined $f_{\text{cut}} \equiv f(\epsilon_{\text{cut}}, \Gamma)$, and $\tau \simeq (2n_{\pm} + n_p)\sigma_T \Delta' = \tau_{\pm}(1 + n_p/2n_{\pm})$ is the optical depth of the emission region. We can also evaluate the pair-to-baryon ratio and the optical depth against pairs as

$$\frac{2n_{\pm}}{n_p} \simeq \left(1 + \frac{16m_p^2 L_{\text{ann}} L_0 f_{\text{cut}}}{3m_e^2 L_p^2} \right)^{1/2} - 1, \quad (16)$$

$$\tau_{\pm} \simeq \frac{m_e L_p}{m_p L_0 f_{\text{cut}}} \left[\left(1 + \frac{16m_p^2 L_{\text{ann}} L_0 f_{\text{cut}}}{3m_e^2 L_p^2} \right)^{1/2} - 1 \right]. \quad (17)$$

Compared to Eqs. (11) and (12), we additionally need information on the amount of baryons L_p to obtain τ , L_{\pm} and τ_{\pm} . If we take the no-pair limit $2n_{\pm} \ll n_p$ in Eqs. (14), (15) and (17), we find that τ does not depend on L_{ann} , and $L_{\pm}, \tau_{\pm} \rightarrow 0$, as expected.

Even if we cannot estimate L_p , we have useful constraints only from pair-signatures. First, we can show

$$\tau_{\pm} < \left(\frac{16}{3} \frac{L_{\text{ann}}}{L_0 f_{\text{cut}}} \right)^{1/2} < \tau. \quad (18)$$

The above inequalities can be derived by exploiting $L_p > 0$ for Eqs. (14) and (17), respectively. Therefore, observations of pair-signatures give us the upper limit on the optical depth against pairs. Especially, we can exclude the pair photospheric emission model when we have $\tau_{\pm} \ll 1$. Second, with $L_p \lesssim L_{\gamma}$, we can observationally give an upper limit on τ as well as lower limits on τ_{\pm} and $2n_{\pm}/n_p$ by replacing L_p with L_{γ} in Eqs. (14), (16) and (17).

3. CASES FOR LIMITED OBSERVATIONS

3.1. The Case of Non-detected Pair-Annihilation Lines

We can gain some information on the fireball even if a pair-annihilation line is not observed. The non-detection of pair-annihilation lines means

$$L_{\text{ann}} \lesssim \epsilon L_{\epsilon}(\epsilon_{\text{ann}}) = L_0 \left(\frac{\Gamma m_e c^2}{(1+z)\epsilon_0} \right)^{2-\beta}. \quad (19)$$

If we can measure L_p , we can give upper limits on τ , $2n_{\pm}/n_p$ and τ_{\pm} by replacing L_{ann} with $L_0(\Gamma m_e c^2/(1+z)\epsilon_0)^{2-\beta}$ in Eqs. (14), (16) and (17).

Even when we cannot estimate L_p , the inequalities (18) where $L_p > 0$ is used, yield the looser constraint on the optical depth against pairs as

$$\tau_{\pm} \lesssim \left[\frac{16}{3 f_{\text{cut}}} \left(\frac{\Gamma m_e c^2}{(1+z)\epsilon_0} \right)^{2-\beta} \right]^{1/2}. \quad (20)$$

If the right hand side of the above inequality is smaller than unity, i.e., $\epsilon_{\text{cut}} \gg [16(\beta-1)/3\xi(\beta)]^{\frac{1}{\beta-1}} [\Gamma/(1+z)] m_e c^2$, we can exclude the pair photospheric emission model. If we use $L_p \lesssim L_{\gamma}$ instead of $L_p > 0$, we obtain an upper limit on τ by replacing L_p and L_{ann} with L_{γ} and $L_0(\Gamma m_e c^2/(1+z)\epsilon_0)^{2-\beta}$, respectively, in Eq. (14).

Note that we have implicitly assumed that Γ is already determined by another means. At least we have $1 \leq \Gamma < (1+z)\epsilon_{\text{cut}}/m_e c^2$. Γ can be estimated from $\tau_{\gamma\gamma}(\epsilon_{\text{cut}}) = 1$ in Eq. (6) if we give the emission radius r . For example, r may be estimated from the frequently used relation $r \approx 2\Gamma^2 c \delta t_{\text{decay}}/(1+z)$, where the decay time of a pulse δt_{decay} is basically determined by the angular spreading time scale (Baring & Harding 1997; Lithwick & Sari 2001). The possible thermal emission component may be also useful to estimate Γ (Pe'er et al. 2007).

3.2. The Case of Non-detected Cutoff Energy

Because of the limited sensitivity of the detector, the observed maximum energy ϵ_{max} may be smaller than the true cutoff energy ϵ_{cut} . As seen in Eq. (10), $f(\epsilon, \Gamma)$ increases with ϵ for $\epsilon \lesssim \epsilon_{\text{cut}}$, as long as the cutoff energy is determined by the pair-creation process. (More precisely, $\tau_{\gamma\gamma}(\epsilon)$, hence $f(\epsilon, \Gamma)$ typically reaches almost the maximum value around $\epsilon \sim \tilde{\epsilon}_{\text{peak}}$ for the low energy spectral index $\alpha \lesssim 1$, where ϵ_{peak} is the peak energy. On the other hand, $\tau_{\gamma\gamma}(\epsilon)$ always increases with ϵ for $\alpha \gtrsim 1$.) Then, we have

$$f(\epsilon_{\text{cut}}, \Gamma) \gtrsim f(\epsilon_{\text{max}}, \Gamma). \quad (21)$$

If we can measure L_p , we can give upper limits on τ and τ_{\pm} as well as an lower limit on $2n_{\pm}/n_p$ by replacing f_{cut} with $f_{\text{max}} \equiv f(\epsilon_{\text{max}}, \Gamma)$ in Eqs. (14), (16) and (17).

Without knowing L_p , the inequalities (18), where $L_p > 0$ is used, yield the looser upper limit on τ_{\pm} as

$$\tau_{\pm} \lesssim \left(\frac{16}{3} \frac{L_{\text{ann}}}{L_0 f_{\text{max}}} \right)^{1/2}. \quad (22)$$

If the right hand side of the above inequality is less than unity, i.e., $\epsilon_{\text{max}} \gg [16(\beta-1)/3\xi(\beta)]^{\frac{1}{\beta-1}} [\Gamma m_e c^2/(1+z)] L_{\text{ann}} L_0^{-1} [\Gamma m_e c^2/(1+z)\epsilon_0]^{2-\beta}$, the pair photospheric emission model is ruled out. If we use $L_p \lesssim L_{\gamma}$ instead of $L_p > 0$, we obtain an upper limit on τ as well as a lower limit on $2n_{\pm}/n_p$ by replacing L_p and f_{cut} with L_{γ} and f_{max} , respectively, in Eqs. (14) and (16).

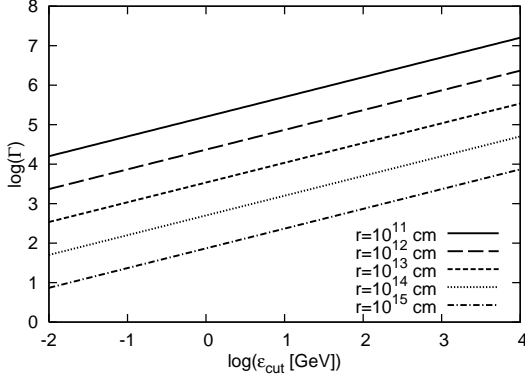


FIG. 4.— The relation between the cutoff energy ε_{cut} and bulk Lorentz factor Γ for given collision radii r . A simple power-law photon spectrum is assumed. Used parameters are $E_0 = 10^{51}$ ergs, $\varepsilon_0 = 10^{2.5}$ keV and $z = 0.1$. Note that $\varepsilon_{\text{cut}} \lesssim \tilde{\varepsilon}_{\text{peak}}$ is also assumed implicitly.

The above arguments in this subsection can be applied even when the fireball is completely thin, i.e., the cutoff energy due to the pair-creation process in the source does not exist. If we know that this is the case from other means, we can replace $f_{\text{max}} \equiv f(\varepsilon_{\text{max}}, \Gamma)$ with $f(\tilde{\varepsilon}_{\text{peak}}, \Gamma)$ in the inequality (21) for $\alpha \lesssim 1$.

4. IMPLICATIONS

In this paper, we have clarified that pair-signatures provide useful information on the fireball in GRBs only with observable quantities. The strategy for acquiring the physical quantities is summarized in the caption of Fig. 1.

4.1. Examination of r and Γ

The determination of emission radii r is important not only for specifying the model of prompt emissions but also for various model-predictions (e.g., neutrino production in the internal shock model is sensitive to emission radii r (e.g., Murase & Nagataki 2006; Murase et al. 2006)). After this work on pair-signatures by us, Gupta & Zhang (2007) recently focused on this issue of the unknown emission radius. They re-expressed the cutoff energy as a function of r and Γ . By using Eqs. (6) and (7), we can see that the emission radius r is obtained from observationally determined ε_{cut} , ε_0 and the radiation energy of a subshell at ε_0 , $E_0 \sim L_0 \delta t_{\text{rise}} / (1+z)$, if we know Γ by other means. Here, δt_{rise} is the rise time of a pulse, which is basically determined by the comoving width of the subshell $\Delta' \approx \Gamma c \delta t_{\text{rise}} / (1+z)$. Eq. (1) is one of the ways to determine Γ . Other means (e.g., by using the photospheric emission component (Pe'er et al. 2007)) are also useful.

On the other hand, the emission radius can be also estimated via the relation $r \approx 2\Gamma^2 c \delta t_{\text{decay}} / (1+z)$, as noted in § 3.1. Once this relation is validated, we can compare the emission radius estimated by using this relation with that determined from ε_{cut} . In other words, we can test whether Γ determined by Eq. (9) and $r \approx 2\Gamma^2 c \delta t_{\text{decay}} / (1+z)$ is consistent with Γ estimated from Eq. (1) and other means or not. Because the derived Γ should be consistent if the emission radius is the same, they will be useful as another closure relation (see § 5). Note that we have not so far assumed the relation $r \approx 2\Gamma \Delta' \approx 2\Gamma^2 c \delta t_{\text{rise}} / (1+z)$, which is expected in the internal shock model but may not be true. In fact, models other than the internal shock model do not always predict $r \approx 2\Gamma \Delta'$, but can lead to $r \gg 2\Gamma \Delta'$.

4.2. Test of the Pair Photospheric Emission Model

As already noted, pair-signatures are especially useful to test the pair photospheric emission model, where the prompt emission comes from $r_{\text{ph}} \approx r_{\text{ph},\pm}$. We can measure τ_{\pm} by Eq. (17) with L_p , and an upper limit on τ_{\pm} by the inequalities (18) without L_p . If we can observe either the pair-annihilation line or the cutoff energy due to pair-creation, an upper limit on τ_{\pm} is obtained by Eq. (17) with the inequalities (19) or (21) for known L_p , and by the inequality (20) or (22) for unknown L_p . When the fireball is pair-dominated, i.e., the inequality (13) is satisfied, we have $\tau \approx \tau_{\pm}$. In addition, under the photospheric emission model, we expect that high-energy gamma-rays are produced by the dissipation around the photosphere (which may occur at the sub-photosphere) and emerge from the emission region at $r \sim r_{\text{ph}}$. Therefore, the pair photospheric emission model predicts $\tau \approx \tau_{\pm} \sim 1$ in Eqs. (11) or (14).

When the fireball is pair-dominated, the photospheric radius where $\tau \approx \tau_{\pm} \approx 1$ can be expressed as

$$r_{\text{ph}} \approx r_{\text{ph},\pm} \approx \frac{f_{\text{cut}} L_0 \sigma_T}{4\pi m_e c^3 \Gamma^3 q}, \quad (23)$$

where $q \equiv r_{\text{ph}} / \Gamma \Delta'$ which is expected to be an order-of-unity factor in the internal shock model. Eq. (23) is essentially the same equation as that shown in Rees & Meszaros (2005). Note that the relation $r \approx 2\Gamma \Delta'$ expected in the internal shock model leads to $q = 2$.

When $L_{\text{ann}} \sim \varepsilon L_{\varepsilon}(\varepsilon_{\text{ann}}) = L_0 [\Gamma m_e c^2 / (1+z) \varepsilon_0]^{2-\beta}$, the pair photospheric emission model, under which we expect $\tau \approx \tau_{\pm} \sim 1$, predicts the unique relation between ε_{cut} and ε_{ann} . Eq. (11) yields (after the integration over ε_{γ} in Eq. (10) which is the expression of f_{cut}),

$$\frac{\varepsilon_{\text{cut}}}{\varepsilon_{\text{ann}}} \sim \left[\frac{(\beta-1)}{\tau_{\pm}^2} \frac{16}{3\xi(\beta)} \right]^{\frac{1}{\beta-1}} \sim \left[(\beta-1) \frac{16}{3\xi(\beta)} \right]^{\frac{1}{\beta-1}}. \quad (24)$$

If pairs are created by the underlying continuum photons, the pair-annihilation line cannot exceed the continuum emission much prominently, i.e., $L_{\text{ann}} \sim L_0 [\Gamma m_e c^2 / (1+z) \varepsilon_0]^{2-\beta}$ (Ioka et al. 2007; Pe'er & Waxman 2004; Pe'er et al. 2006). Therefore, the relation (24) could be satisfied for many bursts under the pair photospheric emission model. Superposing low-quality spectra of many events by adjusting either ε_{ann} or ε_{cut} could help to find the other feature in this model.

5. DISCUSSION

Although the pair-signatures give us useful information, we have to be careful because there are some uncertainties in obtained quantities and we have put several assumptions in deriving equations and inequalities shown in this paper.

First, we have assumed that all the photons come from the same emission region. However, this might not be true. Although we assume the same emission radius for pair-signatures as a first step consideration, actual emissions may not come from the same emission radius. For example, let us consider cases where high-energy gamma-rays come from two different emission radii r_1 and r_2 ($r_1 < r_2$). There will be three possibilities; (A) Case where the observed pair-annihilation line comes from r_1 , while the pair-creation cutoff coming from r_2 , $\varepsilon_{\text{cut},2}$ is higher than that from r_1 , $\varepsilon_{\text{cut},1}$; (B) Case where the observed pair-annihilation line comes from r_2 , while the pair-creation cutoff coming from r_1 , $\varepsilon_{\text{cut},1}$ is higher than that from r_2 , $\varepsilon_{\text{cut},2}$; (C) Case where both of the observed

pair-annihilation line and (higher) pair-creation cutoff come from r_1 or r_2 .

(A-1) Case (A) where the underlying continuum dominantly comes from r_1 at $\varepsilon \lesssim \varepsilon_{\text{cut},1}$; In this case, we will ideally see $\varepsilon_{\text{cut},1}$ coming from r_1 as well as $\varepsilon_{\text{cut},2}$ which is the higher cutoff. Because we have higher $\tau_{\gamma\gamma}$ at smaller r (and/or for larger E_0), with the given Γ , the former cutoff could be naturally lower than the latter. If we could see two ε_{cut} in the photon spectrum (i.e., one is due to $\varepsilon_{\text{cut},1}$, while the other is $\varepsilon_{\text{cut},2}$ which is higher), our recipes would be applied to the line and the lower cutoff $\varepsilon_{\text{cut},1}$. (A-2) Case (A) where the underlying continuum dominantly comes from r_2 at $\varepsilon \lesssim \varepsilon_{\text{cut},2}$; In this case, and if the outflow has similar Γ at the two emission radii, we would expect that time-resolved detailed observations could separate different emission radii. It is because, if we can use $r \approx 2\Gamma^2 c \delta t_{\text{decay}} / (1+z)$, the larger emission radius r leads to the longer δt_{decay} . On the other hand, if the outflow has different Γ at the two emission radii, it is useful to determine Γ independently in various ways. Although it may be observationally difficult, not only the estimation by using Eq. (1) but also other means for estimation (e.g., by using the photospheric emission component and/or the relation $r \approx 2\Gamma^2 c \delta t_{\text{decay}} / (1+z)$), would enable us to evaluate Γ . If emissions come from the same emission radius, we expect that all of the Γ we obtain should be consistent. (B-1) Case (B) where the underlying continuum dominantly comes from r_2 at $\varepsilon \lesssim \varepsilon_{\text{cut},2}$; Since the pair-creation cutoff from r_1 is higher, not completely masked by the underlying continuum from r_2 , we can see $\varepsilon_{\text{cut},2}$ below $\varepsilon_{\text{cut},1}$ as in the case (A-1). We may apply our recipes to the line and the lower cutoff $\varepsilon_{\text{cut},2}$. (B-2) Case (B) where the underlying continuum dominantly comes from r_1 at $\varepsilon \lesssim \varepsilon_{\text{cut},1}$; In this case, the higher cutoff $\varepsilon_{\text{cut},1}$ comes from the inner radius r_1 , while $\varepsilon_{\text{cut},2}$ is masked and the observed pair-annihilation line is generated at the larger radius r_2 . It would require, typically, that the Lorentz factor at the outer emission radius r_2 is smaller than that at the inner emission radius r_1 , because the prominent pair-annihilation line and the lower $\varepsilon_{\text{cut},2}$ would mean copious pairs and photons at r_2 . Therefore, evaluation of Lorentz factors by several means would be important. (C-1) Case (C) where both pair-signatures come from r_1 while the underlying continuum dominantly comes from r_2 at $\varepsilon \lesssim \varepsilon_{\text{cut},2}$; In this case, we can see $\varepsilon_{\text{cut},1}$ above $\varepsilon_{\text{cut},2}$ in principle. Hence, our recipes can be applied to the line and higher cutoff, while if we use the lower cutoff, we could obtain the Lorentz factor that is inconsistent with other estimations. (C-2) Case (C) where both pair-signatures come from r_2 while the underlying continuum dominantly comes from r_1 at $\varepsilon \lesssim \varepsilon_{\text{cut},1}$; Similarly to the case (C-1), we could two ε_{cut} ideally. We can apply our recipes to the higher cutoff, and then obtain the Lorentz factor that is consistent with the estimation by Eq. (1).

Therefore, what we have to do is that we apply our recipes to the time-resolved spectra, if possible, and then compare the Lorentz factors obtained by several means in order to check the consistency. When we have two or more cutoffs, we may select the cutoff that provides the consistent Lorentz factor. Once we can see that emissions come from the same radius, our recipes described in this paper can be used in order to obtain information on the fireball of GRBs

Second, we have assumed that sufficiently relativistic electrons cool down rapidly, $t_{\text{cool}} \ll t_{\text{ann}}$, which is expected in many models (Ioka et al. 2007; Pe'er & Waxman 2004; Pe'er et al. 2005). However, the pair-annihilation line might

come from relativistic pairs. For example, in the slow dissipation scenario (Ghisellini & Celotti 1996), e.g., as might be expected from magnetic reconnection, the typical electron Lorentz factor at the end of the dynamical time γ_{cool} could be larger than unity (Pe'er et al. 2006). If $\gamma_{\text{cool}} > 1$, we should use $\varepsilon_{\text{ann}} \sim \Gamma \gamma_{\text{cool}} m_e c^2 / (1+z)$ instead of Eq. (1), and the expression of L_{ann} should also be modified (where L_{ann} is suppressed for $\gamma_{\text{cool}} \beta_{\text{cool}}^2 / (1+\beta_{\text{cool}}^2) \gtrsim 1$) (Svensson 1982). In such a case, it becomes more difficult to observe the pair-annihilation line since the width of the pair-annihilation line is broadened by more than order-of-unity in energy due to the broad distributions of relativistic pairs, although we may check this observationally (Svensson 1982). If we can specify the distributions of electrons and positrons properly (e.g., thermal distributions), we could evaluate L_{ann} , Γ and the shape of the pair-annihilation line with elaborate observational results in the future. But in the case where the distributions of electrons and positrons are unknown, they are model-dependent as demonstrated in Pe'er et al. (2005,2006), which would cause possible ambiguities for our recipes.

Third, we have also assumed that the cutoff energy ε_{cut} is determined by attenuation via $\gamma\gamma \rightarrow e^+e^-$ in the source. However, the attenuation due to interaction with cosmic infrared background photons should be also taken into account when ε_{cut} is sufficiently high. This cosmic attenuation effect can make it difficult to determine the cutoff energy at the source, ε_{cut} . The observed maximum energy might also represent the maximum energy of accelerated electrons. In order to evaluate ε_{cut} properly, the careful analyses will be needed. The secondary delayed emission may be also useful (Murase et al. 2007). Note that we can apply the recipe in (§ 3.2) even without the true ε_{cut} .

Pair-signatures may be detected by the future-coming GLAST satellite. However, the detection of pair-annihilation lines may be difficult due to line-broadening, as discussed in (§ 2). Lines are observed as bumps, so that evaluated τ and L_{\pm} will have uncertainties by a factor, due to observational difficulties in precise determination of L_{ann} and Γ . In addition, it is hopeful to apply our recipes to single pulses. Some GRBs can be regarded as single pulse events. For example, some bright bursts such as BATSE trigger numbers 647 and 999 exhibited relatively smooth, long, single pulses, which were separated well from other pulses. For such single pulses, we may expect emissions from the approximately same emission radius, although the spectrum also showed the time-dependent evolution. Note that, our recipes could be applied to flares, where wider and smoother pulses are seen (Burrows et al. 2005; Ioka et al. 2005). A flare may come from the approximately same emission radius. However, the detection of pair-annihilation lines will be more difficult observationally because pair-annihilation lines from flares are typically expected at ~ 10 MeV if the Lorentz factor of flare-outflows is ~ 10 . Furthermore, emissions from flares will be contaminated by afterglow components.

The height of the pair-annihilation line may be comparable to the underlying continuum emission. Therefore, we have to collect sufficiently many photons to identify the pair-annihilation line. For example, if the height of the pair-annihilation line is larger than the underlying continuum by a factor ~ 2 , we need to collect ~ 20 photons for the 3σ detection at $\sim \varepsilon_{\text{ann}}$. When the spectrum of the prompt emission is expressed by a power-law extending to sufficiently high energies, GLAST/LAT is expected to find ~ 70 GRBs per year

under the criterion that > 10 photons per bursts are collected for the energy threshold 30 MeV (Omodei et al. 2006). It suggests that, if a significant fraction of GRBs accompanies pair-annihilation lines, we expect good opportunities to see them.

We also have to note that there may be some uncertainties in determining ε_{cut} . Opacity skin effects can sometimes render the exponential attenuation $\exp(-\tau_{\gamma\gamma})$ a poor descriptor of attenuation with $1/(1 + \tau_{\gamma\gamma})$, which leads to broken power-laws rather than exponential turnovers (Baring 2006; Baring & Harding 1997). We expect that such ambiguities could be solved by observing the maximum energy for a lot of events.

We thank S. Nagataki, T. Nakamura and K. Toma for helpful comments. This work is supported in part by the Grant-in-Aid for the 21st Century COE "Center for Diversity and Universality in Physics" from the Ministry of Education, Culture, Sports, Science and Technology (MEXT) of Japan and by the Grant-in-Aid from the Ministry of Education, Culture, Sports, Science and Technology (MEXT) of Japan, No.18740147, No.19047004 (K.I.). K.M. is supported by Grant-in-Aid for JSPS Fellows.

REFERENCES

- Baring, M.G. 2006, *ApJ*, 650, 1004
 Baring, M.G., and Harding, A.K. 1997, *ApJ*, 491, 663
 Burrows, D.N., et al. 2005, *Science*, 309, 1833
 Coppi, P.S., and Blandford, R.D. 1990, *MNRAS*, 245, 453
 Ghisellini, G., and Celotti, A. 1999, *ApJ*, 511, L93
 Gould, R.J., and Schröder, G.P. 1967, *Phys. Rev.*, 155, 1404
 Gupta, N., and Zhang, B. 2007, arXiv:0708.2763
 Ioka, K., Kobayashi, S., and Zhang, B. 2005, *ApJ*, 631, 429
 Ioka, K., Toma, K., Yamazaki, R., and Nakamura, T. 2006, *A&A*, 458, 7
 Ioka, K., Murase, K., Toma, K., Nagataki, S., and Nakamura, T. 2007, *ApJ*, 670, L77
 Lightman, A.P., and Zdziarski, A.A. 1987, *ApJ*, 319, 643
 Lithwick, Y., and Sari, R. 2001, *ApJ*, 555, 540
 Mészáros, P. 2006, *Rev. Prog. Phys.*, 69, 2259
 Murase, K., and Nagataki, S. 2006, *Phys. Rev. D*, 73, 063002
 Murase, K., Ioka, K., Nagataki, S., and Nakamura, T. 2006, *ApJ*, 651, L5
 Murase, K., Asano, K., and Nagataki, S. 2007, *ApJ*, 671, 1886
 Omodei, N., and GLAST/LAT GRB Science Group 2006, in *American Institute of Physics Conference Series*, Vol. 836, *Gamma-Ray Bursts in the Swift Era*, ed. S. S. Holt, N. Gehrels, and J. A. Nousek, 642647
 Pe'er, A., and Waxman, E. 2004, *ApJ*, 613, 448
 Pe'er, A., Mészáros, P., Rees, M. 2005, *ApJ*, 635, 476
 Pe'er, A., Mészáros, P., Rees, M. 2006, *ApJ*, 642, 995
 Pe'er, A., et al. 2007, *ApJ*, 664, L1
 Razzaque, S., Mészáros, P., and Zhang, B. 2004, *ApJ*, 613, 1072
 Rees, M.J., and Mészáros, P. 1994, *ApJ*, 430, L93
 Rees, M.J., and Mészáros, P. 2005, *ApJ*, 628, 847
 Svensson, R. 1982, *ApJ*, 258, 335
 Svensson, R. 1987, *MNRAS*, 227, 403
 Zhang, B., *Chin. J. Astron. Astrophys.*, 7, 1
 Zhang, B., and Mészáros, P. 2001, *ApJ*, 559, 110
 Zhang, B., et al. 2007, *ApJ*, 655, 989